ORIGINAL RESEARCH

Knockout Mice Reveal Key Roles for Claudin 18 in Alveolar Barrier Properties and Fluid Homeostasis

Guanglei Li[1]*, Per Flodby[1]*, Jiao Luo[1], Hidenori Kage[1], Arnold Sipos[1], Danping Gao[1], Yanbin Ji[1], LaMonta L. Beard[1], Crystal N. Marconett[2,3,4], Lucas DeMaio[1], Yong Ho Kim[1], Kwang-Jin Kim[1,5,8,9], Ite A. Laird-Offringa[2,3,4], Parviz Minoo[7], Janice M. Liebler[1], Beiyun Zhou[1], Edward D. Crandall[1,6,10], and Zea Borok[1,3]

[1]Will Rogers Institute Pulmonary Research Center, Division of Pulmonary, Critical Care and Sleep Medicine, Department of Medicine, [2]Department of Surgery, [3]Department of Biochemistry and Molecular Biology, [4]Norris Comprehensive Cancer Center, [5]Department of Physiology and Biophysics, [6]Department of Pathology, and [7]Division of Neonatology, Department of Pediatrics, Keck School of Medicine, University of Southern California, Los Angeles, California; [8]Department of Pharmacology and Pharmaceutical Sciences, School of Pharmacy, University of Southern California, Los Angeles, California; and [9]Department of Biomedical Engineering, and [10]Mork Family Department of Chemical Engineering and Materials Science, Viterbi School of Engineering, University of Southern California, Los Angeles, California

Abstract

Claudin proteins are major constituents of epithelial and endothelial tight junctions (TJs) that regulate paracellular permeability to ions and solutes. Claudin 18, a member of the large claudin family, is highly expressed in lung alveolar epithelium. To elucidate the role of claudin 18 in alveolar epithelial barrier function, we generated claudin 18 knockout (C18 KO) mice. C18 KO mice exhibited increased solute permeability and alveolar fluid clearance (AFC) compared with wild-type control mice. Increased AFC in C18 KO mice was associated with increased β-adrenergic receptor signaling together with activation of cystic fibrosis transmembrane conductance regulator, higher epithelial sodium channel, and Na-K-ATPase (Na pump) activity and increased Na-K-ATPase β1 subunit expression. Consistent with *in vivo* findings, C18 KO alveolar epithelial cell (AEC) monolayers exhibited lower transepithelial electrical resistance and increased solute and ion permeability with unchanged ion selectivity. Claudin 3 and claudin 4 expression was markedly increased in C18 KO mice, whereas claudin 5 expression was unchanged and occludin significantly decreased. Microarray analysis revealed changes in cytoskeleton-associated gene expression in C18 KO mice, consistent with observed F-actin cytoskeletal rearrangement in AEC monolayers. These findings demonstrate a crucial nonredundant role for claudin 18 in the regulation of alveolar epithelial TJ composition and permeability properties. Increased AFC in C18 KO mice identifies a role for claudin 18 in alveolar fluid homeostasis beyond its direct contributions to barrier properties that may, at least in part, compensate for increased permeability.

Keywords: bioelectrical properties; permeability; alveolar fluid clearance; β2-adrenergic receptor; tight junction

In mammals, the alveolar epithelium constitutes a unique interface between air spaces and underlying lung tissue. Lung alveolar epithelial cells (AECs) interconnected by tight junctions (TJs) regulate solute and water transport to maintain alveolar fluid homeostasis, thereby enabling normal gas exchange and protecting the lung from inhaled hazardous agents. TJs are located close to the apical cell surface between adjacent AECs and seal paracellular spaces. TJs are multiprotein complexes that include transmembrane proteins (e.g., claudins, occludin, and junctional adhesion molecules) and

(Received in original form August 7, 2013; accepted in final form February 16, 2014)

*These authors contributed equally to this work.

This work was supported by the Hastings Foundation; by the Whittier Foundation; by National Institutes of Health grants ES017034, HL056590, HL062569, HL089445, HL095349, HL108364, HL114094, HL114959, and NCI CCSG 5P30 CA 014089; by ACS/Canary postdoctoral fellowship #PFTED-10–207–01-SIED (C.N.M); and by Norris Comprehensive Cancer Center core grant P30CA014089 from the National Cancer Institute.

Correspondence and requests for reprints should be addressed to Zea Borok, M.D., Will Rogers Institute Pulmonary Research Center, Division of Pulmonary, Critical Care and Sleep Medicine, Keck School of Medicine, University of Southern California, IRD 723, M/C 9520, Los Angeles, CA 90089-9520. E-mail: zborok@usc.edu

This article has an online supplement, which is accessible from this issue's table of contents at www.atsjournals.org

Am J Respir Cell Mol Biol Vol 51, Iss 2, pp 210–222, Aug 2014

Originally Published in Press as DOI: 10.1165/rcmb.2013-0353OC on March 3, 2014
Internet address: www.atsjournals.org

intracellular accessory proteins (e.g., zonula occludens [ZO] proteins), which link claudins and occludin to the actin cytoskeleton to stabilize TJs (1).

Claudins, constituting a family of 27 known members in the mouse, are important regulators of TJ selectivity and paracellular permeability to ions and solutes (2, 3). The predominant claudins expressed in alveolar epithelium are claudin 18, claudin 3, and claudin 4 (4–6). Other claudins, including claudin 5 and claudin 7, are expressed by AECs at lower levels (4). Different claudin family members have distinct functions and tissue distribution and interact with each other homotypically (i.e., between identical claudins) and heterotypically (i.e., between different claudins) to regulate epithelial barrier properties in a cell- and/or tissue-specific fashion. In the lung, claudin 3 is expressed primarily by alveolar epithelial type II (AT2) cells, and higher expression of claudin 3 was shown to decrease alveolar epithelial barrier function as assessed by transepithelial resistance (R_T) and dye flux measurements (5). Conversely, overexpression of claudin 4 increased R_T in AEC monolayers compared with control monolayers (5). Claudin 5 is highly expressed in pulmonary endothelium, whereas epithelial expression is low (7). Claudin 5 has been suggested to contribute to sealing between lung endothelial cells (8); however, increased claudin 5 expression in AECs is associated with leakier TJs (9). These studies highlight the fact that individual claudin members demonstrate properties that are highly context dependent and that TJ properties are determined by the precise composition of claudin family members in a given cell type.

High expression of claudin 18 (*Cldn18*) has been described in lung and stomach epithelium (10, 11), with lung-specific (C18.1) and stomach-specific (C18.2) isoforms of claudin 18 regulated by alternative promoter usage. Deletion of C18.2 in knockout (KO) mice was reported to result in the loss of TJ strands and increased paracellular H^+ leak in the stomach (12, 13). Recent studies of bone formation in claudin 18 KO (C18 KO) mice indicate a role for this gene as a negative regulator of bone resorption and osteoclast differentiation (14). Claudin 18 is specifically expressed in lung epithelial cells, whereas no expression is found in lung endothelium (7). In distal lung, claudin 18 is expressed in alveolar epithelial type I (AT1) and AT2 cells, with higher levels in AT1 cells in rats (6). Although the specific role of claudin 18 in alveolar epithelium is unknown, increased claudin 18 localization to the cell membrane was associated with higher R_T in cultured rat AECs (15). Given that AT1 cells constitute $>$ 95% of alveolar surface area and express claudin 18 at high levels, these findings imply a potentially important role for this claudin in the regulation of lung barrier function, although its specific role in alveolar homeostasis has not been evaluated in C18 KO mice.

To elucidate the role of claudin 18 in alveolar epithelium, we generated mice with ubiquitous KO of the *Cldn18* gene by crossing floxed claudin 18 mice to a cytomegalovirus promoter-driven Cre (CMV-Cre) deleter strain. Although C18 KO mice do not manifest respiratory dysfunction at baseline, they demonstrate increased alveolar epithelial permeability and alveolar fluid clearance (AFC), whereas AEC monolayers from C18 KO mice show decreased R_T and increased permeability to ions and solutes, suggesting a central nonredundant role for claudin 18 in the regulation of alveolar barrier function and fluid homeostasis.

Materials and Methods

Further details are provided in the online supplement.

Generation of Cldn18 KO Mice

Mice harboring a floxed *Cldn18* allele ($Cldn18^{F/F}$) were generated and crossed to *CMV-cre deleter* mice, resulting in animals with ubiquitous KO of *Cldn18*. Animal protocols were approved by the Institutional Animal Care and Use Committee (IACUC) at the University of Southern California.

Microarray Analysis of Human and Mouse Gene Expression

Analysis of gene expression in human AEC transdifferentiation was recently described (16). Whole lung gene expression analysis of wild-type (WT) versus C18 KO mice was performed using the Illumina MouseRef8 v2 platform (Illumina, San Diego, CA). Data are available in Table E3 in the online supplement and under GEO record GSE48443.

Mouse AT2 Cell Isolation and AEC Monolayer Preparation

Primary AT2 cells were isolated from mouse lungs, and mouse AEC monolayers (MAECMs) were prepared and cultured as previously described (17) with modifications of laminin coating and media serum concentration.

AFC

Mice were anesthetized and instilled intratracheally with PBS with 5% BSA (Sigma-Aldrich, Saint Louis, MO) and 0.25 mg/ml of BSA-Alexa Fluor 594 conjugate as tracer (Life Technologies, Grand Island, NY). Alveolar fluid was aspirated after 30 minutes, fluorescent signals in instillate and aspirate were measured, and AFC was calculated as the ratio between signals in aspirate and instillate.

MAECM Bioelectric Properties

R_T ($k\Omega \cdot cm^2$) and spontaneous potential difference (PD, mV) were measured between Days 4 and 6 in culture using a volt-ohmmeter (EVOM; World Precision Instruments, Sarasota, FL). Equivalent short-circuit current (I_{EQ}, $\mu A/cm^2$) was calculated as $I_{EQ} = PD/R_T$. Ion permeability was determined from dilution and bi-ionic potentials measured across MAECMs.

In Vitro and *In Vivo* Permeability Assays

In vitro MAECM permeability in the apical-to-basolateral direction was determined using 5-carboxyfluorescein (molecular weight [MW] 376 Da) (Life Technologies) and tetramethylrhodamine-isothiocyanate-dextran (TRITC-dextran [average MW, 155,000 Da]; Sigma-Aldrich). Permeability *in vivo* was determined by tail vein injection of 10 mg/kg of fluorescein-BSA (Life Technologies), with measurements of fluorescence in bronchoalveolar lavage fluid (BALF) and serum 2 hours later.

RNA Isolation, RT-PCR, and qRT-PCR

Methods and primers are described in the online supplement.

Western Blot Analysis

Methods and antibodies are described in the online supplement.

Immunofluorescence and Confocal Microscopy

Methods and antibodies are described in the online supplement.

ATPase Activity Assay of Whole Lung Membranes

ATPase hydrolytic activity was determined based on detection of inorganic phosphate (P_i) using the Fiske method (18). Specific Na-K-ATPase activity was calculated based on ouabain-inhibitable activity. Activity was corrected for initial protein amount and expressed as μmol P_i/h/mg protein. Details are provided in the online supplement.

Ventilator-Induced Lung Injury

Details are provided in the online supplement.

Statistical Analysis

Data are shown as means ± SEM. Significance ($P < 0.05$) for ⩾ 3 group means was determined by one-way ANOVA, followed by *post hoc* procedures based on modified Student-Newman-Keuls tests. Two group means were compared for significance using Student's *t* tests. Z-tests were used to determine if ratiometric (i.e., normalized) data were different from control.

Results

Generation and Verification of C18 KO Mice

We generated and verified ubiquitous C18 KO in C18 KO mice as described in detail in the online supplement and as shown in Figure E1.

Higher AFC in C18 KO Mice

AFC was 2.1 times greater in C18 KO mice (48.4 ± 4.5%/h; $n = 5$) than in WT mice (23.1 ± 1.9%/h; $n = 5$) at baseline ($P < 0.001$) (Figure 1A, *left columns*). AFC of WT and C18 KO mice decreased significantly after administration of amiloride ($P < 0.05$ for WT; $P < 0.01$ for C18 KO), an inhibitor of epithelial sodium channels (ENaCs) (Figure 1A, *middle columns*). Although inhibition of AFC was proportional between genotypes, amiloride-sensitive AFC in absolute terms was greater in C18 KO mice, suggesting increased expression and/or activity of ENaCs in KO lung. AFC of WT and C18 KO mice increased significantly with the β2-adrenergic agonist terbutaline ($P < 0.01$ for WT; $P < 0.001$ for C18 KO) (Figure 1A, *right columns*). Terbutaline stimulated AFC proportionally in WT and C18 KO mice, but the effect was larger in absolute terms in the KOs. To further investigate the role of β-adrenergic receptor (βAR) signaling in mediating differences between genotypes, we measured AFC in the presence of propranolol, a βAR inhibitor. The

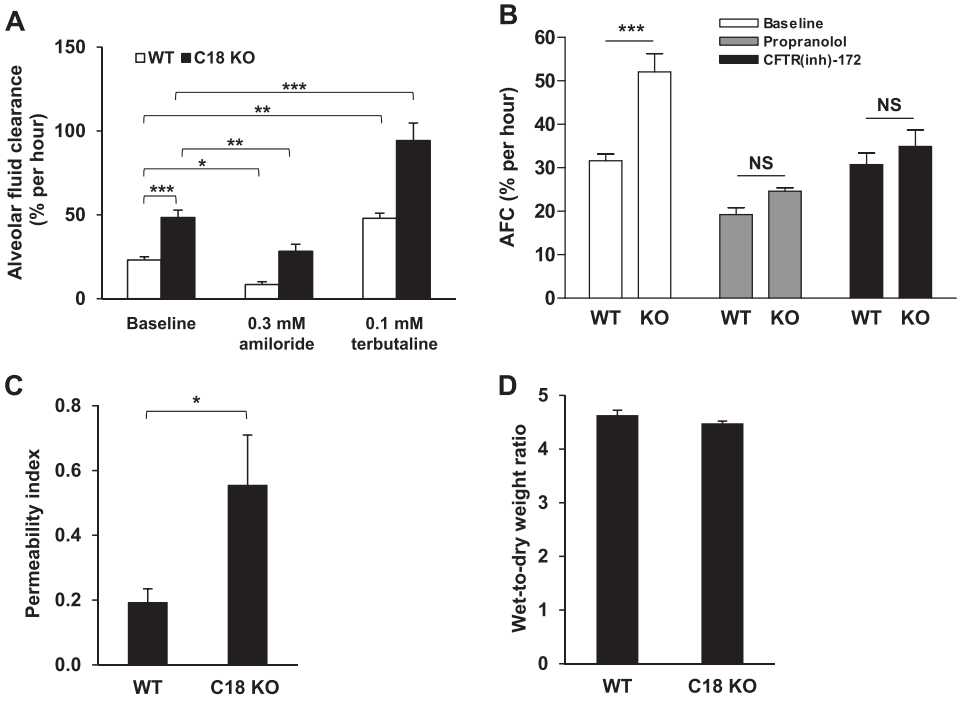

Figure 1. Increased alveolar fluid clearance (AFC) and lung permeability in claudin 18 knockout (C18 KO) mice. (*A*) AFC in C18 KO mice ($n = 5$) was about 2-fold higher than in wild-type (WT) mice ($n = 5$) at baseline (48.4 ± 4.5%/h versus 23.1 ± 1.9%/h; ***$P < 0.001$). Amiloride (0.3 mM) decreased AFC significantly in WT (*$P < 0.05$) and C18 KO (**$P < 0.01$) mice compared with mice of the same genotype at baseline. Terbutaline (0.1 mM) increased AFC significantly in WT (**$P < 0.01$) and C18 KO mice (***$P < 0.001$) compared with mice of the same genotype at baseline. (*B*) In a separate set of experiments, AFC at baseline was 52.1 ± 4.2%/h in C18 KO mice ($n = 3$) versus 31.6 ± 1.6%/h in WT mice ($n = 3$) (***$P < 0.001$). In the presence of the β-adrenergic receptor antagonist propranolol, there was no significant difference (NS) in AFC between C18 KO mice (24.6 ± 0.8%/h; $n = 3$) versus WT mice (19.2 ± 1.6%/h; $n = 3$). CFTR(inh)-172 decreased AFC to 34.9 ± 3.9%/h in C18 KO mice ($n = 3$) versus 30.7 ± 2.7%/h in WT mice ($n = 3$), a difference that was not significant. (*C*) *In vivo* permeability index of fluorescein-BSA from blood into alveolar spaces in C18 KO mice was significantly higher (0.56 ± 0.15; $n = 9$) than in WT mice (0.19 ± 0.04; $n = 6$). *$P < 0.05$. (*D*) Wet-to-dry lung weight ratios of WT and C18 KO mice were similar (4.63 ± 0.54 [$n = 34$] in WT mice versus 4.48 ± 0.23 [$n = 33$] in C18 KO mice; $P = 0.14$).

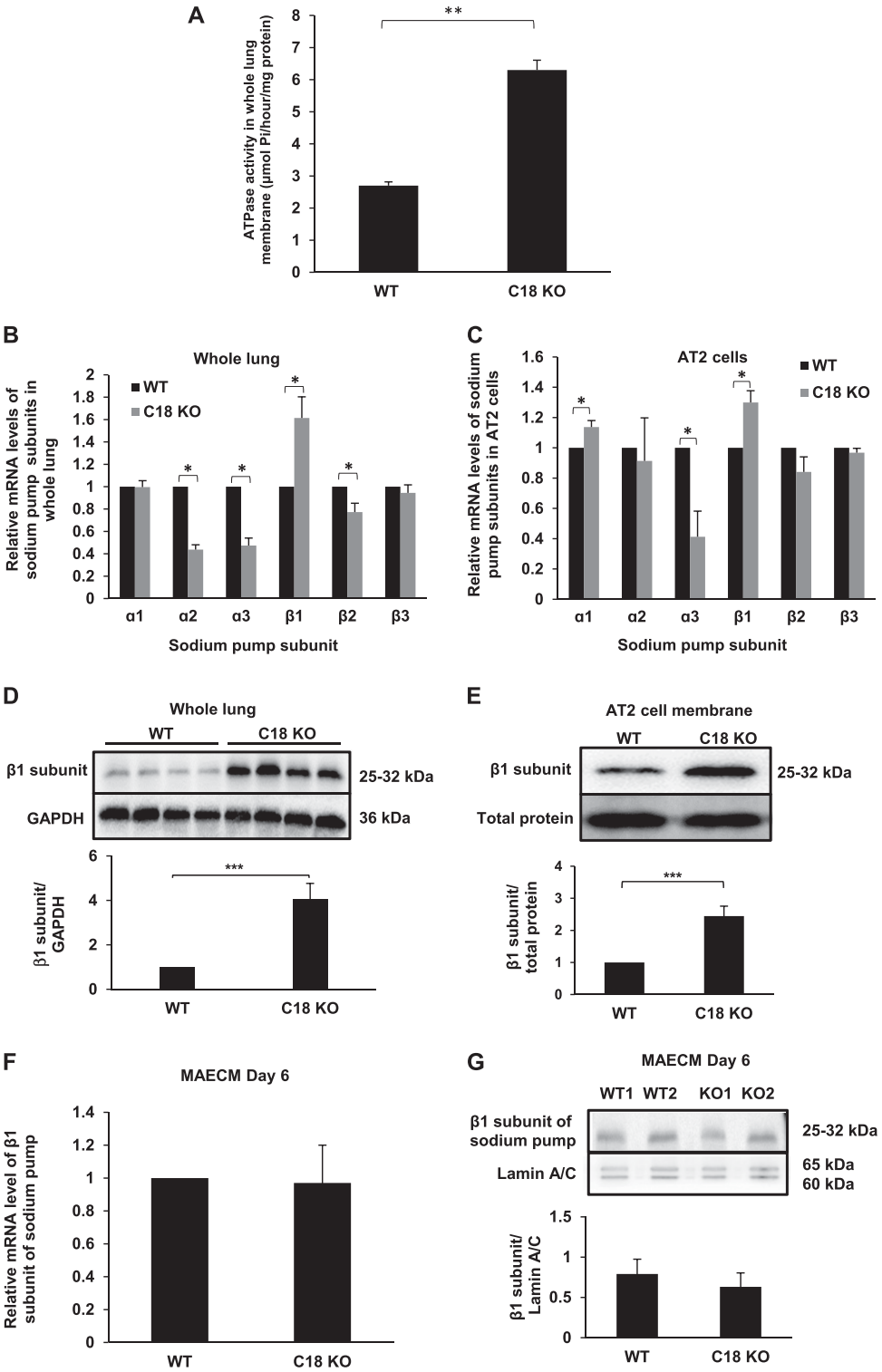

Figure 2. Increased Na-K-ATPase activity and β1 subunit expression in C18 KO mice. (*A*) Ouabain-sensitive ATPase activity (attributed primarily to Na-K-ATPase activity) was significantly higher (2.3-fold; $^{**}P < 0.01$) in whole lung membranes from C18 KO (6.3 ± 0.31; $n = 3$) versus WT mice (2.7 ± 0.12; $n = 3$). (*B*) Quantitative RT-PCR (qRT-PCR) analysis of WT and C18 KO whole lung demonstrates relative expression of Na pump subunits (expression level of WT = 1.0). In C18 KO mice, expression of the β1 subunit increased by 61%, whereas α2, α3, and β2 subunits decreased by 56, 53, and 23%, respectively ($^{*}P < 0.05$). Expression of α1 and β3 subunits remained unchanged. (*C*) qRT-PCR analysis of Na pump subunit gene expression in freshly isolated AT2 cells from C18 KO mice demonstrates increased expression of β1 and α1 subunits of 30 and 14%, respectively, whereas the α3 subunit was decreased ($^{*}P < 0.05$) and α2, β2, and β3 subunits were unchanged compared with WT mice. (*D*) Western blot analysis

difference in AFC between C18 KO and WT mice was largely eliminated by propranolol (Figure 1B), suggesting that increased βAR signaling underlies higher AFC in C18 KO mice. Previous studies have provided evidence for a role of CFTR in βAR-stimulated AFC (19, 20). To test for involvement of CFTR, we measured AFC in the presence of the inhibitor CFTR(inh)-172, which had only a small effect on AFC in WT mice (Figure 1B), consistent with previous studies (21), but a significant effect on AFC in C18 KO mice, which decreased to levels similar to WT mice. These CFTR inhibitor experiments suggest that increased βAR signaling in C18 KO lungs activates CFTR, resulting in higher ion transport and AFC. We investigated if increased βAR signaling is accompanied by increased expression of the β2-adrenergic receptor (β2AR) protein in C18 KO lungs. Although there was a trend toward higher levels of β2AR protein in C18 KO whole lung samples, the difference did not achieve statistical significance (Figure E3A), suggesting that increased total β2AR protein level was not the main cause for elevated βAR signaling. Although *Cftr* mRNA expression was increased in C18 KO lung 3.35-fold by microarray (Table E3) and 5.88-fold by qRT-PCR (Figure E3B), CFTR protein levels were not different between genotypes (Figure E3C), suggesting that increased CFTR activity in C18 KO lung is the result of higher ion channel activity in response to increased β-adrenergic signaling.

Normal Wet-to-Dry Lung Weight Ratios in C18 KO Mice Despite Increased Solute Permeability

To measure lung permeability *in vivo*, fluorescein-BSA was injected via tail vein with subsequent measurement of fluorescent signal levels in BALF. The absence of claudin 18 resulted in a 2.9-fold increase in lung permeability index in C18 KO versus WT mice (0.56 ± 0.15 [$n = 9$] versus 0.19 ± 0.04 [$n = 6$], respectively; $P < 0.05$) (Figure 1C). Despite higher permeability in C18 KO lungs, no difference between genotypes in wet-to-dry lung weight ratios was found (Figure 1D), likely due to higher AFC in KO mice.

Increased Na-K-ATPase Activity and β1 Subunit Expression in C18 KO Mice

We observed a 2.3-fold increase ($P < 0.01$) in ouabain-sensitive ATPase activity in whole lung cell membrane preparations from C18 KO versus WT mice, consistent with increased Na-K-ATPase activity in lungs of C18 KO mice (Figure 2A). By qRT-PCR, the level of Na-K-ATPase β1 subunit mRNA was significantly increased by 61% ($P < 0.05$) in C18 KO lungs, whereas expression of α1 and β3 subunits was unchanged (Figure 2B). The α2, α3, and β2 subunits were significantly decreased ($P < 0.05$) in C18 KO lungs, although these changes are likely of low functional significance given the low lung expression of these subunits. In isolated AT2 cells, expression of β1 subunit was increased 30% and α1 subunit by 14%, whereas α3 subunit decreased (all $P < 0.05$) (Figure 2C). Western blot analysis showed increased β1 subunit protein in whole lung (4.1-fold; $P < 0.001$) (Figure 2D) and AT2 cell membranes (2.4-fold; $P < 0.001$) (Figure 2E). Higher Na pump expression and activity most likely contributed to increased AFC in C18 KO mice. In contrast, analysis of β1 subunit mRNA and protein expression in MAECMs revealed no differences between C18 KO and WT cells (Figures 2F and 2G).

Increased Ion and Solute Permeability in MAECMs Derived from C18 KO Mice

We further characterized the role of claudin 18 in the permeability properties of alveolar epithelium using MAECMs derived from C18 KO versus WT mice. R_T on Day 6 was significantly lower in MAECMs from C18 KO mice (Figure 3A), indicating increased transepithelial ion permeability *in vitro*. In contrast, active ion transport was unchanged in monolayers from C18 KO mice, as indicated by similar I_{EQ} in both genotypes (Figure 3B), consistent with the observation of no difference in β1 subunit expression between C18 KO and WT MAECMs (Figure 2F and 2G). We measured permeability to solutes of two different sizes, 5-carboxyfluorescein (MW, 376 Da) and TRITC-dextran (average MW, 155,000 Da), in MAECMs from WT and C18 KO mice. C18 KO monolayers exhibited significantly higher permeability to 5-carboxyfluorescein and TRITC-dextran (Figures 3C and 3D) compared with WT monolayers. No differences between genotypes were found in permeability ratios for Na and Cl ions (P_{Na}/P_{Cl}) and for Na and K ions (P_{Na}/P_K) (Figures 3E and 3F). However, calculated Na^+, K^+, and Cl^- permeabilities were higher across C18 KO compared with WT MAECMs (Figure 3G), consistent with decreased R_T. These data suggest a major role for claudin 18 in TJ function in MAECMs.

Effects of C18 KO on Expression of other Claudins and Occludin

Expression of claudin 3 mRNA in whole lung was 1.8-fold higher ($P < 0.05$) in C18 KO versus WT mice (Figure 4A). Western blot analysis demonstrated increased expression of claudin 3 protein in C18 KO mice in whole lung lysates (1.83-fold increase [$n = 4$]; $P < 0.001$) (Figure 4B) and in AT2 cell membrane fractions (1.75-fold increase [$n = 3$]; $P < 0.05$) (Figure 4C). Staining for claudin 3 in MAECMs (Day 6) showed that loss of claudin 18 leads to up-regulation of claudin 3 at the cell membrane in AT1-like cells (Figure 4D). Expression of claudin 4 mRNA was increased in C18 KO lung (3.99-fold increase [$n = 3$]; $P < 0.05$) (Figure 4E). Claudin 4 protein levels in C18 KO lungs or MAECMs were not determined due to lack of specificity of all antibodies tested. Claudin 5 protein levels in freshly isolated AT2 cell membranes were unchanged in C18 KO mice (Figure 4F). Expression of occludin was 42% lower ($P < 0.001$) in C18 KO versus WT lung (Figure 4G), and decreased occludin membrane localization was observed in MAECMs (Figure 4H) despite unchanged occludin mRNA (data not shown).

Figure 2. (Continued). of whole lung for β1 Na pump subunit demonstrates about 4-fold greater protein levels in C18 KO versus WT mice. ***$P < 0.001$. GAPDH, glyceraldehyde 3-phosphate dehydrogenase. (*E*) Western blot analysis of AT2 cell membrane fractions shows significantly higher (2.4-fold) β1 subunit expression in C18 KO versus WT mice. ***$P < 0.001$. (*F*) Analysis of β1 mRNA levels in mouse alveolar epithelial cell monolayers (MAECMs) on Day 6 in culture shows no differences between genotypes. (*G*) Western blot analysis of whole cell lysates from Day 6 MAECMs demonstrates that β1 protein level is unchanged in C18 KO versus WT mice.

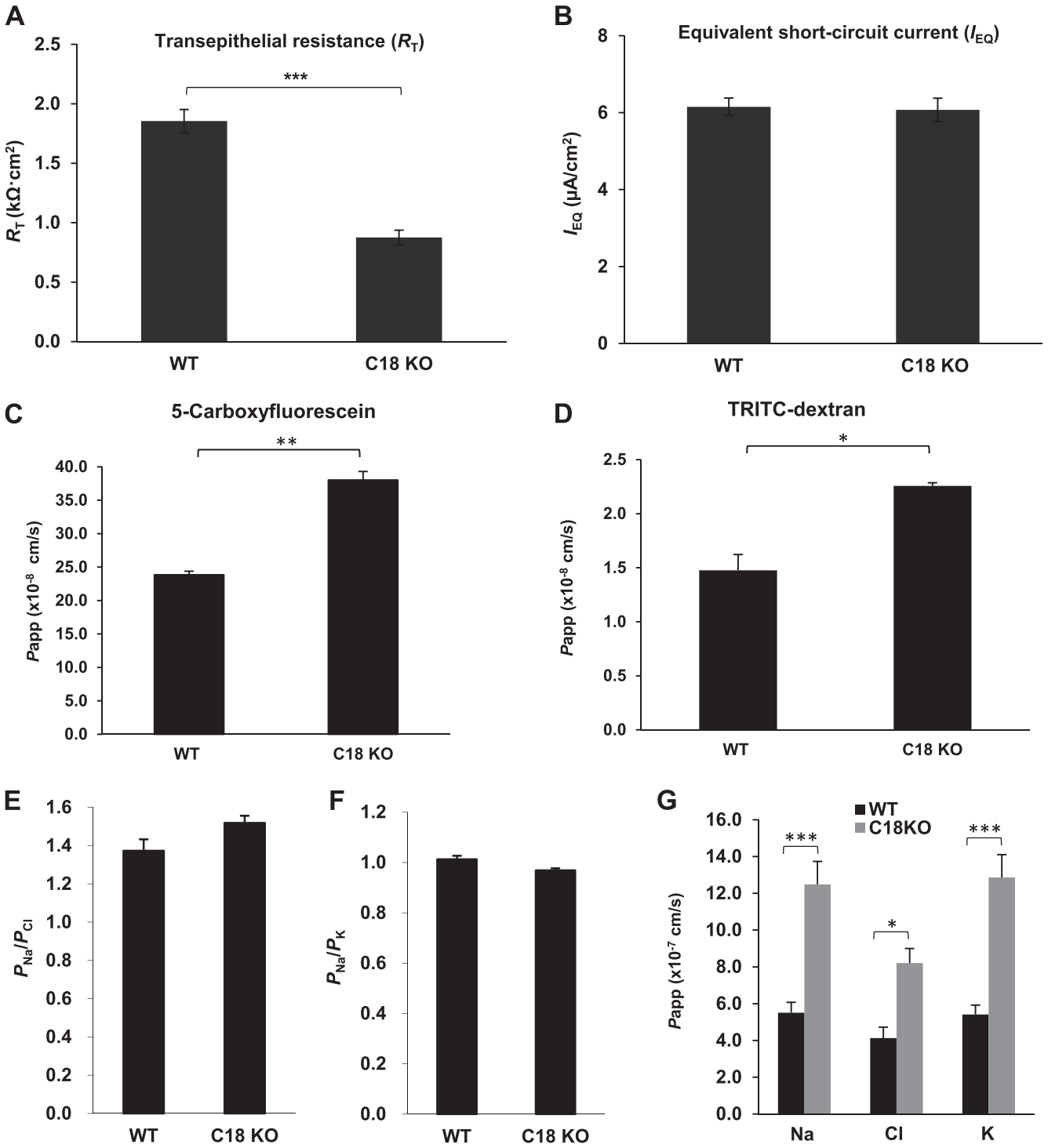

Figure 3. Decreased transepithelial electrical resistance (R_T) and increased solute and ion permeability in MAECMs from C18 KO mice. (*A*) R_T was significantly lower across MAECMs from C18 KO mice (0.88 ± 0.06 kΩ·cm^2; n = 53) versus MAECMs from WT mice (1.86 ± 0.10 kΩ·cm^2; n = 51). ***$P < 0.001$. (*B*) There was no difference in I_{EQ} between C18 KO (6.1 ± 0.3 μA/cm^2; n = 53) and WT (6.2 ± 0.2 μA/cm^2; n = 51) MAECMs. (*C*) *In vitro* permeability (*P*app) to 5-carboxyfluorescein of MAECMs from C18 KO mice ($38 \times 10^{-8} \pm 1.3 \times 10^{-8}$ cm/s; n = 3) was significantly higher versus MAECMs from WT mice ($24 \times 10^{-8} \pm 0.5 \times 10^{-8}$ cm/s; n = 3). **$P < 0.01$. (*D*) *In vitro* tetramethylrhodamine-isothiocyanate (TRITC)-dextran permeability (*P*app) was significantly higher in MAECM from C18 KO mice ($2.3 \times 10^{-8} \pm 0.03 \times 10^{-8}$ cm/s; n = 3) versus MAECM from WT mice ($1.5 \times 10^{-8} \pm 0.15 \times 10^{-8}$ cm/s; n = 3). *$P < 0.05$. (*E*) P_{Na}/P_{Cl} was not different between WT (1.37 ± 0.06; n = 7) and C18 KO (1.52 ± 0.04; n = 7) MAECM. (*F*) No difference in P_{Na}/P_K was found between genotypes (1.01 ± 0.01 versus 0.97 ± 0.01 in WT [n = 7] and C18 KO [n = 7] MAECMs, respectively). (*G*) Ion permeability was significantly higher in C18 KO compared with WT MAECMs (n = 7) for Na (***$P < 0.001$), Cl (*$P < 0.05$), and K (***$P < 0.001$).

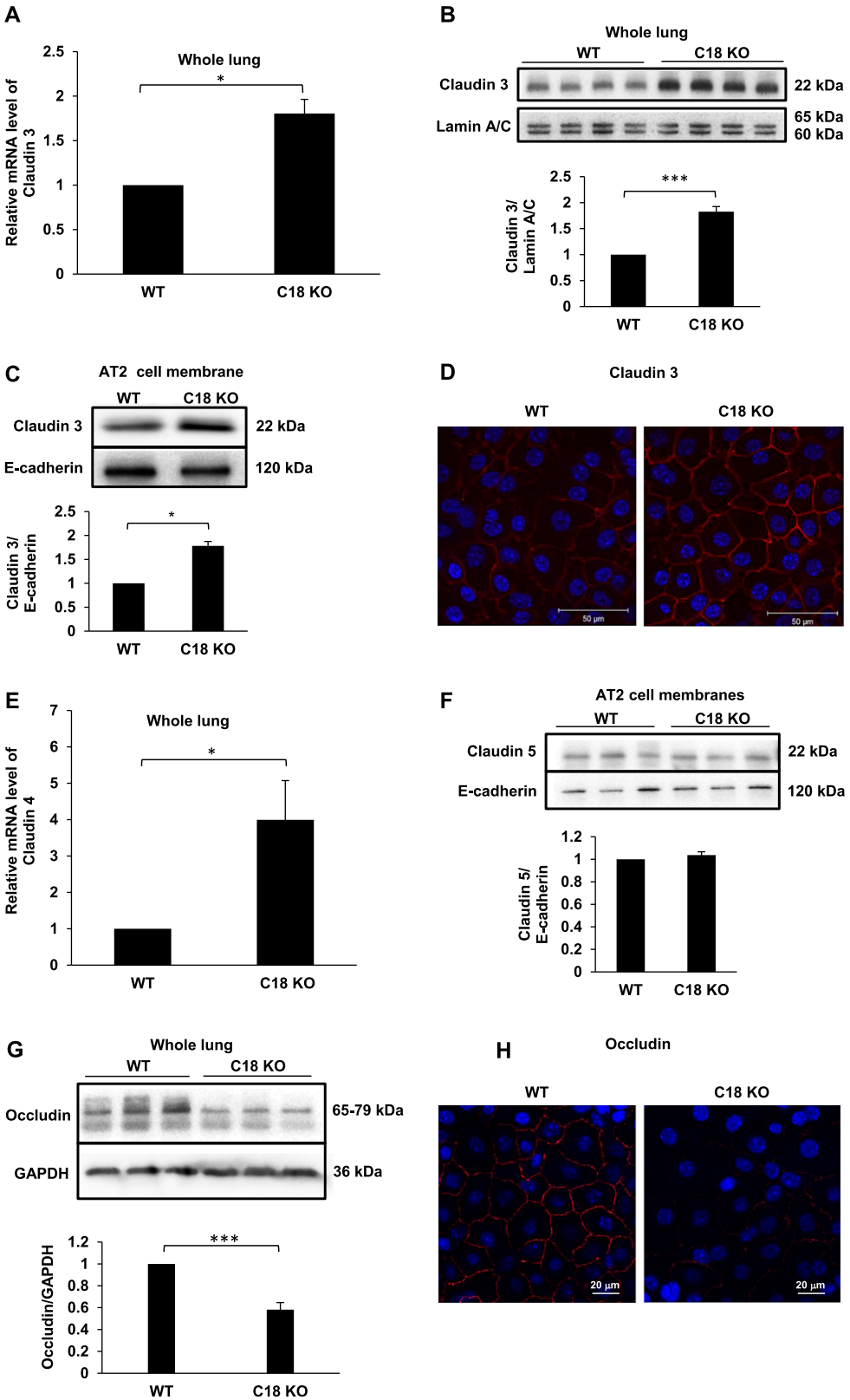

Figure 4. Increased claudin and decreased occludin expression in C18 KO lungs and alveolar epithelial cells. (*A*) qRT-PCR analysis of whole lung shows that expression of claudin 3 mRNA is 1.8-fold higher in C18 KO versus WT mice. *$P < 0.05$. (*B*) Western blot analysis of whole lung demonstrates significantly greater (~ 2-fold) expression of claudin 3 protein in C18 KO versus WT mice. ***$P < 0.001$. (*C*) Western blot analysis shows significantly greater (~ 2-fold) expression of claudin 3 protein in freshly isolated AT2 cell membrane fractions derived from C18 KO versus WT mice. *$P < 0.05$. (*D*)

Changes in other TJ-Associated Proteins in C18 KO Mice

ZO-1 and ZO-2 are cytoplasmic TJ proteins that directly bind transmembrane TJ proteins (e.g., claudins and occludin), adherens junction proteins, and the cytoskeleton. No difference in expression of ZO-1 or ZO-2 protein between WT and C18 KO mice was detected in whole lung or whole lung membranes by Western blot analysis (Figures 5A and 5B). We observed increased separation of ZO-1 between neighboring AECs of C18 KO mice (Figures 5C and E4). The separation distance in C18 KO mice was increased 77.0 ± 1.2% compared with WT mice ($P < 0.05$) (Figure 5D). Increased separation of ZO-2 was also evident in C18 KO monolayers (Figure E5). ZO-1 and claudin 3 were colocalized, consistent with TJ separation rather than with changes in subcellular localization of ZO-1 or ZO-2 proteins (Figure E6). These results suggest alterations in TJ and intercellular adhesion in monolayers formed by claudin 18–deficient AECs.

Cytoskeletal Changes in C18 KO Lungs and AECs

We performed microarray gene expression analysis of whole lung RNA from WT and C18 KO mice, followed by Ingenuity Pathway Analysis. Unsupervised hierarchical clustering revealed that the most variant genes allowed perfect distinction between WT and C18 KO mice (Figure E7). Differential gene expression analysis between WT and C18 KO whole lung revealed 145 genes (163 probes) with > 2-fold change in gene expression (Figure 6A; Table E3). Pathway analysis of the 145 genes by Ingenuity Pathway Analysis revealed changes to a number of cellular pathways in C18 KO lung. The most significantly altered pathway in C18 KO lung was the actin cytoskeleton and associated genes (Figure 6B); this finding is potentially important because normal TJs are stabilized by connection to the cytoskeleton via intracellular accessory proteins (mainly ZO proteins), which link claudins and occludin to F-actin (1). Other pathways significantly altered by claudin 18 depletion include cellular adhesion, Rho signaling, and TJ signaling. We used phalloidin staining to visualize F-actin in MAECMs, noting increased phalloidin staining intensity along the plasma membrane of AECs from C18 KO mice compared with WT control mice, with lower cytoplasmic staining intensity (Figure 6C). In some C18 KO cells, we observed perinuclear actin aggregates from which radial fibers projected toward and connected with the cell plasma membrane (Figure 6D), supporting the notion of cytoskeletal rearrangements in C18 KO cells.

Lower Sensitivity to Ventilator-Induced Lung Injury in C18 KO Mice

To investigate the consequences of acute lung injury in mice deficient in claudin 18, we subjected C18 KO and WT control mice to ventilator-induced lung injury (VILI). Total protein concentration in BALF was used as a measure of injury after 3 hours of volume-based VILI. There were no differences between genotypes in BALF protein levels in naive mice or in animals ventilated under noninjurious conditions (Figure 7A). In contrast, injurious ventilation resulted in significantly lower BALF protein levels in C18 KO mice (0.53 ± 0.06 mg/ml) compared with WT mice (1.02 ± 0.27 mg/ml), indicating that C18 KO mice are less sensitive to VILI. No significant differences in BAL cell concentrations or in percent macrophages were found between genotypes (data not shown), which may be due to the short time span (3 h) of ventilation. Pressure-based VILI experiments yielded similar results (data not shown). VILI has been shown to be attenuated in *Egr1*−/− KO mice (22). Our microarray analysis demonstrated that expression of *Egr1* was decreased 14.0-fold in C18 KO mice (Table E3), and this finding was confirmed by qRT-PCR, which showed a 22.5-fold decrease in lungs of C18 KO mice (Figure 7B). These results suggest that decreased *Egr1* expression is likely an important factor contributing to lower sensitivity to VILI in C18 KO mice.

Discussion

We generated mice with KO of *Cldn18*, a gene encoding the TJ protein claudin 18, which is highly expressed in AECs, particularly in AT1 cells (6). C18 KO mice did not exhibit apparent respiratory dysfunction at baseline. Despite increased lung solute permeability, KO mice had unchanged wet-to-dry weight ratios at baseline. Absence of edema was most likely due to the fact that AFC was substantially increased in C18 KO mice, associated with higher β-adrenergic signaling, increased CFTR and ENaC activity, and elevated ouabain-sensitive ATPase activity. Expression of the Na-K-ATPase β1 subunit in whole lung and AT2 cell membranes was increased in C18 KO mice, whereas no statistically significant changes in β2AR and CFTR protein expression were found. MAECMs lacking claudin 18 manifested lower R_T and higher transepithelial ion and solute permeability. Changes in expression of several components of the TJ complex were detected in lungs of C18 KO mice, where expression of claudin 3 and claudin 4 increased and occludin decreased, whereas ZO-1 and ZO-2 levels were unchanged. Antibody staining of C18 KO MAECMs for ZO-1 and ZO-2 showed increased distance between stained domains in neighboring cells, the result of increased TJ separation as evidenced by claudin 3/ZO-1 double staining. Microarray analysis revealed that the most significantly altered pathway in C18 KO lungs was the actin cytoskeleton, a result supported by increased localization of F-actin along cell membranes in C18 KO MAECMs. These findings demonstrate a crucial nonredundant role for claudin 18 in regulation of alveolar epithelial TJ composition and alveolar fluid homeostasis.

Figure 4. (Continued). Antibody staining for claudin 3 shows greater expression and membrane localization in C18 KO MAECM on Day 6 (confocal micrographs). (*E*) qRT-PCR analysis demonstrates significantly higher (~ 4-fold) claudin 4 mRNA expression in C18 KO versus WT lungs. *$P < 0.05$. (*F*) Western blot analysis of claudin 5 expression in AT2 cell membranes demonstrates similar expression in WT and C18 KO mice. (*G*) Western blot analysis of occludin protein expression shows a significant decrease in whole lung samples from C18 KO mice. ***$P < 0.001$. (*H*) Confocal microscopy demonstrates lower levels of occludin localized at tight junctions in MAECMs derived from C18 KO mice.

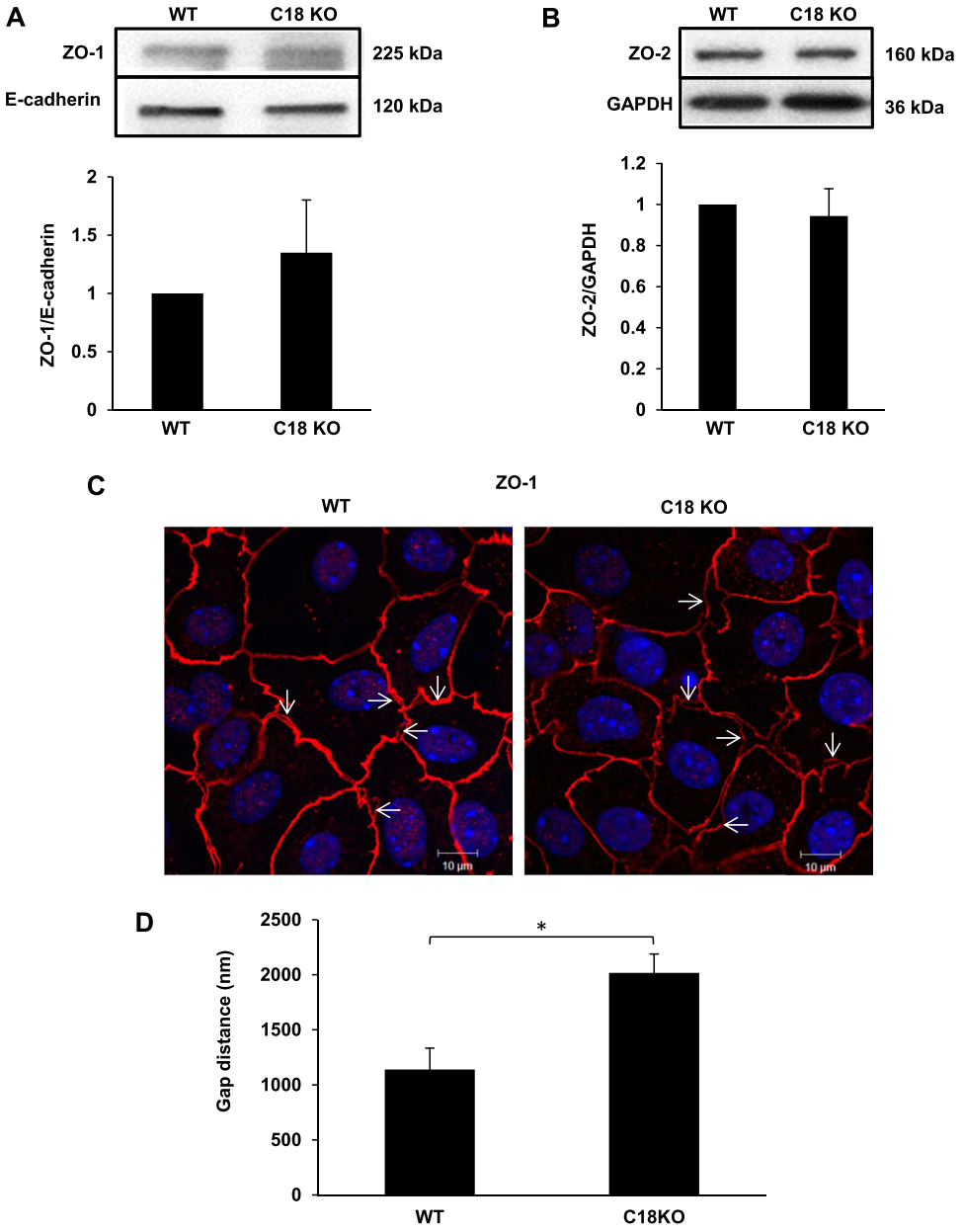

Figure 5. Zonula occludens (ZO)-1 and ZO-2 expression and localization in WT and C18 KO mice. (*A* and *B*) Western blot analysis of whole lung membrane fractions for ZO-1 (*A*) and ZO-2 (*B*) shows similar expression levels in WT and C18 KO mice. (*C*) Immunofluorescence and confocal microscopy reveal increased distance between ZO-1 localization in adjacent cells in MAECMs from C18 KO compared with WT mice on Day 10 (confocal micrographs). *Arrows* indicate examples of gaps. (*D*) The distance between ZO-1 staining in adjacent alveolar epithelial cells was significantly higher in C18 KO compared with WT MAECM. *$P < 0.05$.

Increased Permeability of Alveolar Epithelium in C18 KO Mice

C18 KO mice have higher permeability to fluorescein-BSA, suggesting an important barrier function for claudin 18 *in vivo*. Claudin 18–deficient MAECMs exhibit lower R_T, higher ion permeability (K^+, Na^+, and Cl^-), and higher permeability to small (5-carboxyfluorescein) and large (TRITC-dextran) solutes compared with MAECMs from WT mice. This alveolar epithelial barrier dysfunction suggests a unique role for claudin 18 in AEC TJ formation and maintenance that is not compensated by other claudins or TJ-associated proteins. KO of the stomach-specific form of claudin 18 (claudin 18.2) led to increased H^+, Na^+, and Cl^- permeability (12), similar to the increase in ion permeability found in AECs in this study, although there was a slight increase in Na^+ versus Cl^- selectivity in stomach epithelium that was not observed in AECs. Permeability to solutes (biotin and 4 kDa dextran) was unchanged in C18 KO stomach epithelial cells, although we observed increased permeability to small and large solutes in MAECMs. These data indicate context-dependent regulation of TJ properties by claudin 18.

Increased AFC and β-Adrenergic Signaling in C18 KO Mouse Lungs

C18 KO mice showed considerably higher AFC than WT mice, reflecting increased active ion transport in alveolar epithelium despite increased permeability (23). The increase in AFC in response to β-adrenergic stimulation by terbutaline was higher in C18 KO mice in absolute terms, indicating a greater capacity to respond via βAR. AFC in C18 KO mice was inhibited by the βAR inhibitor propranolol, further implicating βAR signaling in increased AFC. Inhibition of CFTR largely eliminated AFC differences between genotypes, consistent with previous studies implicating βAR signaling in the up-regulation of AFC via activation of CFTR (19, 20). Although *Cftr* mRNA expression was increased, we did not find differences in CFTR protein levels between genotypes, suggesting that increased CFTR activity in C18 KO lung is based on increased activity per channel. This suggests a scenario whereby elevated β-adrenergic signaling results in increased levels of cAMP, activation of protein kinase A, and phosphorylation/activation of CFTR, leading to chloride absorption and resultant increases in sodium and water absorption. Amiloride-sensitive portions of AFC were similar in C18 KO and WT mice. However, because the rate of AFC is higher in C18 KO mice, amiloride-sensitive AFC is larger in absolute terms in the KO mice, suggesting higher numbers and/or increased activity (higher open probability) of amiloride-sensitive ENaCs in C18 KO lung. The importance of the Na pump in AFC has been directly demonstrated by increased AFC after overexpression of Na pump subunits (24–28). β-Adrenergic signaling has been reported to increase transcription and translation of Na pump subunit genes (29) and to mobilize intracellular Na pumps for insertion into the basolateral cell plasma membrane (30), making β-adrenergic signaling a plausible mechanism underlying increased expression of Na pump subunit mRNA and higher ouabain-sensitive ATPase activity observed in C18 KO lungs. These results suggest that elevated β2-adrenergic signaling in C18 KO mice results in increased CFTR, ENaC and Na pump activity, and higher AFC. Increased Na pump protein levels might also be related to the observed cytoskeletal rearrangements in C18 KO AECs. In this regard, plasma

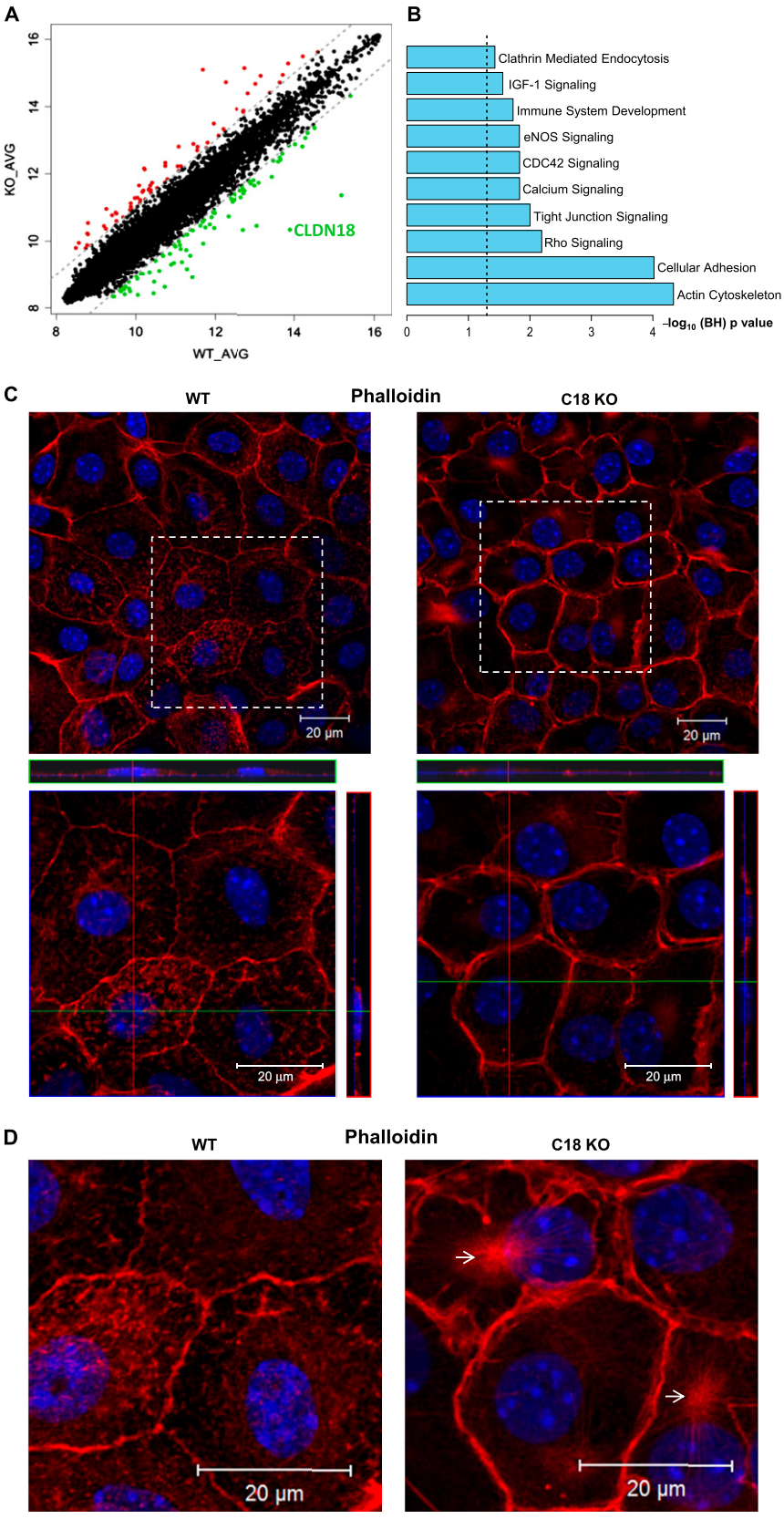

Figure 6. (See figure legend on following page)

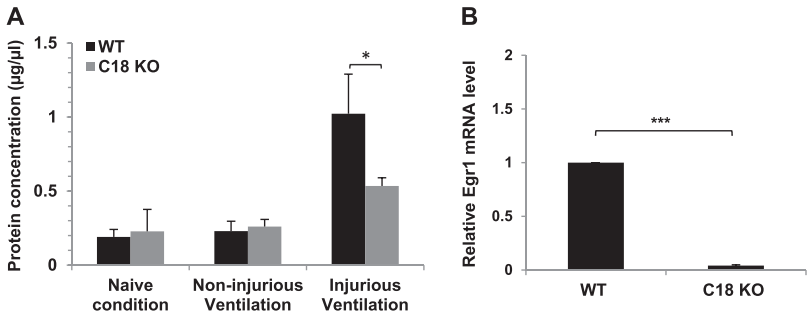

Figure 7. Decreased sensitivity of C18 KO mice to ventilator-induced lung injury. (*A*) Protein concentration in bronchoalveolar lavage (BAL) fluid was measured in untreated (naive) mice and in mice ventilated under noninjurious or injurious conditions. Under injurious conditions, BAL protein concentration in WT mice was significantly (*$P < 0.05$) higher (1.02 ± 0.27 mg/ml; $n = 3$) compared with C18 KO mice (0.53 ± 0.06 mg/ml; $n = 3$). (*B*) qRT-PCR analysis in whole lung shows a 22.5-fold decrease in *Egr1* mRNA expression levels in C18 KO mice (***$P < 0.001$).

membrane-associated proteins α-adducin and ankyrin directly interact with Na pumps (31–35) and are known to regulate cytoskeletal dynamics (36, 37). Although this possibility remains to be investigated, alterations in expression or localization of α-adducin and ankyrin as a result of cytoskeletal rearrangements could affect Na pump expression.

Mechanisms Underlying Increased βAR Signaling and AFC

The fact that C18 KO mice were more resistant to VILI makes it likely that observed changes in AFC are more than just compensatory to increased epithelial permeability because compensatory mechanisms would not be expected to provide a protective advantage. Despite higher AFC and increased ATPase activity in lung membranes and higher expression of the Na-K-ATPase β1 subunit in isolated AT2 cells, no differences in I_{EQ} or expression of the β1 subunit were observed between genotypes in MAECMs, likely due to lack of catecholamines in our serum-free culture conditions. In addition to possible increases in circulating catecholamines, observed cytoskeletal changes could alter cellular responsiveness to β-adrenergic signaling. In this regard, an important function for the cytoskeleton has been demonstrated during internalization and recycling of the β2AR protein (38). Although we did not investigate increased expression of β1AR protein in C18 KO lung, higher β-adrenergic signaling via this receptor remains possible (39).

Changes in Expression/Localization of other TJs and TJ-Associated Proteins

Although decreased TJ localization of claudin 18 could account for the observed increases in epithelial permeability (40), changes in other TJ and TJ-associated proteins could contribute. Increased expression of claudin 3 in TJs was recently shown to decrease R_T and to increase permeability in rat AEC monolayers (5), suggesting that the observed increase in claudin 3 expression in MAECMs from our C18 KO mice may have contributed to compromised barrier properties. Analysis of claudin 4 showed higher mRNA expression in C18 KO lung. Although claudin 4 has been suggested to decrease ion permeability (5, 41, 42), this increase in claudin 4 was unable to overcome the effects of claudin 18 deficiency. Increased expression of claudin 5 in rat AEC monolayers has been associated with higher epithelial permeability and lower R_T (9), but we did not observe changes in claudin 5 expression in membrane fractions from freshly isolated AT2 cells. Expression of occludin, believed to be important in regulating TJ solute permeability (43), was significantly lower in C18 KO lungs, and localization of occludin at the cell membrane was decreased in MAECMs, which may also have contributed to increased permeability in C18 KO lungs. Expression of ZO-1 and ZO-2 protein in C18 KO mice was similar to WT by Western blot analysis. Antibody staining of MAECMs for ZO-1 or ZO-2, as well as double staining for ZO-1/claudin 3, revealed increased separation between stained domains in neighboring cells in C18 KO MAECMs, indicating disruption of cell–cell interactions due to loss of claudin 18. These results demonstrate a nonredundant role for claudin 18 in maintaining the structural and functional integrity of TJs.

Links between TJs and Changes in Rho Signaling, Cytoskeletal Arrangement, and Permeability

The F-actin cytoskeleton is closely associated with TJs and plays a critical role in regulating structural and functional properties of apical cell junctions (44). Despite this known interdependence, precise molecular interactions that serve to stabilize the connection between the cytoskeleton and TJ proteins are poorly understood (37). MAECMs from C18 KO mice demonstrated marked cytoskeletal reorganization, as evidenced by increased localization of F-actin along the cell border as well as perinuclear aggregates and radial F-actin fibers emanating from these aggregates that appear to connect to the plasma membrane. These findings are similar to those observed in models of calcium depletion leading to disassembly of the apical junctional complex and mediated by increased F-actin turnover (45). This F-actin pattern also resembles what has previously been reported in podocytes subjected to experimental mechanical stress and may be secondary to disruption of TJ function as seen in

Figure 6. Cytoskeletal changes in C18 KO lungs and airway epithelial cells. (*A*) Log2 expression of genes in WT (*x* axis) versus C18 KO (*y* axis) mice. *Green* = genes down-regulated ⩾ 2-fold; *red* = genes up-regulated ⩾ 2-fold in C18 KO lung. (*B*) Ingenuity Pathway Analysis. Length of bars in graph indicates $-\log_{10}$ of Benjamini-Hochburg (BH) corrected *P* value for enrichment of indicated pathway. The *dotted line* indicates the threshold border of significance for enriched pathways. (*C*) Confocal micrographs show increased localization of F-actin to the plasma membrane in C18 KO MAECMs by phalloidin staining. Areas magnified and shown in the *lower panels* are indicated by rectangles. *Lower panels* show z-stacks and distinct F-actin staining close to the plasma membrane in C18 KO cells. (*D*) Z-max image (combined fluorescent signal in all z-planes) demonstrating perinuclear F-actin aggregates (indicated by *arrows*) and radial fibers.

our KO mice (46). In that study, stress-induced reorganization of F-actin was prevented by Rho kinase inhibition, suggesting a role for Rho activation in the cytoskeletal changes observed in C18 KO cells. Higher Rho activity affects the cytoskeleton via Rho-associated kinase–mediated phosphorylation of cytoskeletal regulatory components (47), which can result in increased paracellular permeability (48). Rho activity is regulated by guanine-exchange factors (e.g., GEF-H1) that can be sequestered by TJ proteins (e.g., cingulin) (49). TJs can thereby negatively regulate Rho activity and indirectly affect cytoskeletal organization and paracellular permeability. Changes in TJ composition in C18 KO mice might therefore affect the ability of TJs to sequester GEF-H1 and other factors involved in Rho regulation. In addition, microarray analysis indicated that pathways involving the cytoskeleton, Rho and TJs signaling were the most affected in C18 KO lung, indicating important interactions between TJs and the cytoskeleton at a transcriptional level and through altered protein–protein interactions. Further analysis is needed to delineate how altered gene expression in C18 KO lungs affects cytoskeletal organization and TJ composition.

Mechanisms Underlying Decreased Sensitivity of C18 KO Mice to VILI

Despite higher lung permeability, C18 KO mice are less sensitive to VILI compared with WT mice as judged by lower BAL protein concentrations. Microarray and qRT-PCR gene expression analysis revealed a large decrease in expression of the transcription factor *Egr-1* in C18 KO lungs. EGR-1 activates expression of the gene encoding prostaglandin E synthase, an enzyme that increases synthesis of prostaglandin E2, which exacerbates inflammation and lung injury by activating pulmonary prostaglandin E receptor subtype 1 (22). Accordingly, *Egr-1* KO mice feature significantly lower levels of injury in response to VILI (22), suggesting that lower *Egr-1* expression in C18 KO mice is protective. Previous studies have suggested that β-agonists enhance adherens junctions and integrin-mediated cell adhesion (50). Thus, increased β-adrenergic signaling in C18 KO mice might result not only in increased AFC but also in stabilization of cell adhesion, which could contribute to greater protection from stretch-induced lung injury during VILI despite TJ-mediated changes in ion and solute permeability.

Summary

Analysis of the lungs of mice lacking claudin 18 demonstrates a key nonredundant role for this claudin in determining structural and functional integrity of TJ in alveolar epithelium. Together with increased epithelial permeability and cytoskeletal reorganization, C18 KO mice demonstrate higher levels of AFC associated with elevated βAR signaling and increases in CFTR, ENaC, and Na-K-ATPase activities. These studies indicate a major role for claudin 18 in regulating alveolar epithelial barrier properties and fluid homeostasis and suggest that the mechanisms underlying these roles involve interactions with other claudins and TJ-associated proteins as well as effects on cytoskeletal arrangement and expression of cytoskeleton-associated genes. ■

Author disclosures are available with the text of this article at www.atsjournals.org.

Acknowledgments: The authors thank Ray Alvarez for performing mouse AT2 cell preparations; Drs. Nancy Wu, Linda Liu, and Robert Maxson from the Transgenic/Knockout Rodent Core Facility at USC Norris Comprehensive Cancer Center for expert advice and for culturing and electroporation of mouse embryonic stem cells and blastocyst injections; Dr. Chih-Lin Hsieh, USC Department of Urology, for karyotyping targeted embryonic stem cell clones; and Dr. Gokhan Mutlu for generously sharing a protocol for AFC measurements in mice. Histology and microscopy services were provided by the Cell and Tissue Imaging Core of the USC Research Center for Liver Diseases (NIH P30 DK048522 and S10 RR022508).

References

1. Tsukita S, Furuse M, Itoh M. Multifunctional strands in tight junctions. *Nat Rev Mol Cell Biol* 2001;2:285–293.
2. Flodby P, Borok B, Crandall ED, Kim KJ. Claudins and Barrier Function of the Lung. In: Yu ASL, editor. Claudins. Philadelphia: Elsevier; 2010. pp. 177–194.
3. Van Itallie CM, Anderson JM. Claudins and epithelial paracellular transport. *Annu Rev Physiol* 2006;68:403–429.
4. Chen SP, Zhou B, Willis BC, Sandoval AJ, Liebler JM, Kim KJ, Ann DK, Crandall ED, Borok Z. Effects of transdifferentiation and EGF on claudin isoform expression in alveolar epithelial cells. *J Appl Physiol (1985)* 2005;98:322–328.
5. Mitchell LA, Overgaard CE, Ward C, Margulies SS, Koval M. Differential effects of claudin-3 and claudin-4 on alveolar epithelial barrier function. *Am J Physiol Lung Cell Mol Physiol* 2011;301:L40–L49.
6. LaFemina MJ, Rokkam D, Chandrasena A, Pan J, Bajaj A, Johnson M, Frank JA. Keratinocyte growth factor enhances barrier function without altering claudin expression in primary alveolar epithelial cells. *Am J Physiol Lung Cell Mol Physiol* 2010;299:L724–L734.
7. Ohta H, Chiba S, Ebina M, Furuse M, Nukiwa T. Altered expression of tight junction molecules in alveolar septa in lung injury and fibrosis. *Am J Physiol Lung Cell Mol Physiol* 2012;302:L193–L205.
8. Armstrong SM, Wang C, Tigdi J, Si X, Dumpit C, Charles S, Gamage A, Moraes TJ, Lee WL. Influenza infects lung microvascular endothelium leading to microvascular leak: role of apoptosis and claudin-5. *PLoS ONE* 2012;7:e47323.
9. Fernandez AL, Koval M, Fan X, Guidot DM. Chronic alcohol ingestion alters claudin expression in the alveolar epithelium of rats. *Alcohol* 2007;41:371–379.
10. Niimi T, Nagashima K, Ward JM, Minoo P, Zimonjic DB, Popescu NC, Kimura S. Claudin-18, a novel downstream target gene for the T/EBP/NKX2.1 homeodomain transcription factor, encodes lung- and stomach-specific isoforms through alternative splicing. *Mol Cell Biol* 2001;21:7380–7390.
11. Türeci O, Koslowski M, Helftenbein G, Castle J, Rohde C, Dhaene K, Seitz G, Sahin U. Claudin-18 gene structure, regulation, and expression is evolutionary conserved in mammals. *Gene* 2011;481: 83–92.
12. Hayashi D, Tamura A, Tanaka H, Yamazaki Y, Watanabe S, Suzuki K, Suzuki K, Sentani K, Yasui W, Rakugi H, *et al*. Deficiency of claudin-18 causes paracellular H+ leakage, up-regulation of interleukin-1β, and atrophic gastritis in mice. *Gastroenterology* 2012;142:292–304.
13. Tamura A, Yamazaki Y, Hayashi D, Suzuki K, Sentani K, Yasui W, Tsukita S. Claudin-based paracellular proton barrier in the stomach. *Ann N Y Acad Sci* 2012;1258:108–114.
14. Linares GR, Brommage R, Powell DR, Xing W, Chen ST, Alshbool FZ, Lau KH, Wergedal JE, Mohan S. Claudin 18 is a novel negative regulator of bone resorption and osteoclast differentiation. *J Bone Miner Res* 2012;27:1553–1565.
15. Koval M, Ward C, Findley MK, Roser-Page S, Helms MN, Roman J. Extracellular matrix influences alveolar epithelial claudin expression and barrier function. *Am J Respir Cell Mol Biol* 2010;42:172–180.

16. Marconett CN, Zhou B, Rieger ME, Selamat SA, Dubourd M, Fang X, Lynch SK, Stueve TR, Siegmund KD, Berman BP, *et al*. Integrated transcriptomic and epigenomic analysis of primary human lung epithelial cell differentiation. *PLoS Genet* 2013;9:e1003513.
17. Demaio L, Tseng W, Balverde Z, Alvarez JR, Kim KJ, Kelley DG, Senior RM, Crandall ED, Borok Z. Characterization of mouse alveolar epithelial cell monolayers. *Am J Physiol Lung Cell Mol Physiol* 2009; 296:L1051–L1058.
18. Fiske CH, Subbarow Y. The colorimetric determination of phosphorus. *J Biol Chem* 1925;66:375–400.
19. Fang X, Fukuda N, Barbry P, Sartori C, Verkman AS, Matthay MA. Novel role for CFTR in fluid absorption from the distal airspaces of the lung. *J Gen Physiol* 2002;119:199–207.
20. Mutlu GM, Adir Y, Jameel M, Akhmedov AT, Welch L, Dumasius V, Meng FJ, Zabner J, Koenig C, Lewis ER, *et al*. Interdependency of β-adrenergic receptors and CFTR in regulation of alveolar active Na^+ transport. *Circ Res* 2005;96:999–1005.
21. Factor P, Mutlu GM, Chen L, Mohameed J, Akhmedov AT, Meng FJ, Jilling T, Lewis ER, Johnson MD, Xu A, *et al*. Adenosine regulation of alveolar fluid clearance. *Proc Natl Acad Sci USA* 2007;104: 4083–4088.
22. Ngiam N, Peltekova V, Engelberts D, Otulakowski G, Post M, Kavanagh BP. Early growth response-1 worsens ventilator-induced lung injury by up-regulating prostanoid synthesis. *Am J Respir Crit Care Med* 2010;181:947–956.
23. Matthay MA, Clerici C, Saumon G. Invited review: active fluid clearance from the distal air spaces of the lung. *J Appl Physiol (1985)* 2002;93: 1533–1541.
24. Factor P, Dumasius V, Saldias F, Brown LA, Sznajder JI. Adenovirus-mediated transfer of an Na^+/K^+-ATPase β1 subunit gene improves alveolar fluid clearance and survival in hyperoxic rats. *Hum Gene Ther* 2000;11:2231–2242.
25. Thome U, Chen L, Factor P, Dumasius V, Freeman B, Sznajder JI, Matalon S. Na,K-ATPase gene transfer mitigates an oxidant-induced decrease of active sodium transport in rat fetal ATII cells. *Am J Respir Cell Mol Biol* 2001;24:245–252.
26. Azzam ZS, Dumasius V, Saldias FJ, Adir Y, Sznajder JI, Factor P. Na, K-ATPase overexpression improves alveolar fluid clearance in a rat model of elevated left atrial pressure. *Circulation* 2002;105:497–501.
27. Adir Y, Factor P, Dumasius V, Ridge KM, Sznajder JI. Na,K-ATPase gene transfer increases liquid clearance during ventilation-induced lung injury. *Am J Respir Crit Care Med* 2003;168:1445–1448.
28. Machado-Aranda D, Adir Y, Young JL, Briva A, Budinger GRS, Yeldandi AV, Sznajder JI, Dean DA. Gene transfer of the Na^+, K^+-ATPase β1 subunit using electroporation increases lung liquid clearance. *Am J Respir Crit Care Med* 2005;171:204–211.
29. Minakata Y, Suzuki S, Grygorczyk C, Dagenais A, Berthiaume Y. Impact of β-adrenergic agonist on Na^+ channel and Na^+-K^+-ATPase expression in alveolar type II cells. *Am J Physiol* 1998;275: L414–L422.
30. Mutlu GM, Factor P. Alveolar epithelial β2-adrenergic receptors. *Am J Respir Cell Mol Biol* 2008;38:127–134.
31. Lecuona E, Sun H, Chen J, Trejo HE, Baker MA, Sznajder JI. Protein kinase A-Iα regulates Na,K-ATPase endocytosis in alveolar epithelial cells exposed to high CO_2 concentrations. *Am J Respir Cell Mol Biol* 2013;48:626–634.
32. Efendiev R, Krmar RT, Ogimoto G, Zwiller J, Tripodi G, Katz AI, Bianchi G, Pedemonte CH, Bertorello AM. Hypertension-linked mutation in the adducin α-subunit leads to higher AP2-μ2 phosphorylation and impaired Na^+,K^+-ATPase trafficking in response to GPCR signals and intracellular sodium. *Circ Res* 2004;95:1100–1108.
33. Torielli L, Tivodar S, Montella RC, Iacone R, Padoani G, Tarsini P, Russo O, Sarnataro D, Strazzullo P, Ferrari P, *et al*. α-Adducin mutations increase Na/K pump activity in renal cells by affecting constitutive endocytosis: implications for tubular Na reabsorption. *Am J Physiol Renal Physiol* 2008;295:F478–F487.
34. Thevananther S, Kolli AH, Devarajan P. Identification of a novel ankyrin isoform (Ank_G190) in kidney and lung that associates with the plasma membrane and binds α-Na, K-ATPase. *J Biol Chem* 1998;273: 23952–23958.
35. Woroniecki R, Ferdinand JR, Morrow JS, Devarajan P. Dissociation of spectrin-ankyrin complex as a basis for loss of Na-K-ATPase polarity after ischemia. *Am J Physiol Renal Physiol* 2003;284:F358–F364.
36. Baines AJ. Evolution of spectrin function in cytoskeletal and membrane networks. *Biochem Soc Trans* 2009;37:796–803.
37. Naydenov NG, Ivanov AI. Spectrin-adducin membrane skeleton: a missing link between epithelial junctions and the actin cytoskeletion? *BioArchitecture* 2011;1:186–191.
38. Shumay E, Gavi S, Wang HY, Malbon CC. Trafficking of β2-adrenergic receptors: insulin and β-agonists regulate internalization by distinct cytoskeletal pathways. *J Cell Sci* 2004;117:593–600.
39. Gu X, Wang Z, Xu J, Maeda S, Sugita M, Sagawa M, Toga H, Sakuma T. Denopamine stimulates alveolar fluid clearance via cystic fibrosis transmembrane conductance regulator in rat lungs. *Respirology* 2006;11:566–571.
40. Fang X, Neyrinck AP, Matthay MA, Lee JW. Allogeneic human mesenchymal stem cells restore epithelial protein permeability in cultured human alveolar type II cells by secretion of angiopoietin-1. *J Biol Chem* 2010;285:26211–26222.
41. Wray C, Mao Y, Pan J, Chandrasena A, Piasta F, Frank JA. Claudin-4 augments alveolar epithelial barrier function and is induced in acute lung injury. *Am J Physiol Lung Cell Mol Physiol* 2009;297:L219–L227.
42. Van Itallie C, Rahner C, Anderson JM. Regulated expression of claudin-4 decreases paracellular conductance through a selective decrease in sodium permeability. *J Clin Invest* 2001;107:1319–1327.
43. Günzel D, Fromm M. Claudins and other tight junction proteins. *Compr Physiol* 2012;2:1819–1852.
44. Rodgers LS, Fanning AS. Regulation of epithelial permeability by the actin cytoskeleton. *Cytoskeleton (Hoboken)* 2011;68:653–660.
45. Ivanov AI, McCall IC, Parkos CA, Nusrat A. Role for actin filament turnover and a myosin II motor in cytoskeleton-driven disassembly of the epithelial apical junctional complex. *Mol Biol Cell* 2004;15: 2639–2651.
46. Endlich N, Kress KR, Reiser J, Uttenweiler D, Kriz W, Mundel P, Endlich K. Podocytes respond to mechanical stress in vitro. *J Am Soc Nephrol* 2001;12:413–422.
47. Samarin SN, Ivanov AI, Flatau G, Parkos CA, Nusrat A. Rho/Rho-associated kinase-II signaling mediates disassembly of epithelial apical junctions. *Mol Biol Cell* 2007;18:3429–3439.
48. Benais-Pont G, Punn A, Flores-Maldonado C, Eckert J, Raposo G, Fleming TP, Cereijido M, Balda MS, Matter K. Identification of a tight junction-associated guanine nucleotide exchange factor that activates Rho and regulates paracellular permeability. *J Cell Biol* 2003;160:729–740.
49. Balda MS, Matter K. Tight junctions and the regulation of gene expression. *Biochim Biophys Acta* 2009;1788:761–767.
50. Winter MC, Shasby SS, Ries DR, Shasby DM. PAR2 activation interrupts E-cadherin adhesion and compromises the airway epithelial barrier: protective effect of β-agonists. *Am J Physiol Lung Cell Mol Physiol* 2006;291:L628–L635.